

Special
Collection

Cooperativity in Hydrogen-Bonded Macrocycles Derived from Nucleobases

David Almacellas,^[a] Stephanie C. C. van der Lubbe,^[b] Alice A. Grosch,^[b] Iris Tsagri,^[b] Pascal Vermeeren,^{*[b]} Célia Fonseca Guerra,^{*[b]} and Jordi Poater^{*[a, c]}

Introducing a rigid linear π -conjugated acetylene linker into a supramolecular building block consisting of a hydrogen-bond donor side and a hydrogen-bond acceptor side yields a decrease in cooperativity in the resulting formed quartet. This follows from our Kohn-Sham molecular orbital and Voronoi deformation density analyses of hydrogen-bonded macrocycles based on guanine and cytosine nucleobases. The acetylene linker abstracts electron density from the hydrogen-bond

acceptor and donor, making the hydrogen-bond acceptor more negatively charged and the hydrogen-bond donor more positively charged and hence suppressing the donor–acceptor charge transfer interaction between the interacting fragments. This, ultimately, hampers the cooperativity in the hydrogen-bonded macrocycle. We envision that these findings could open the door to new design principles for the development of novel hydrogen-bond supramolecular macrocycles.

Introduction

Molecular recognition and self-assembly are employed in supramolecular chemistry with the aim of developing innovative materials departing from molecular building blocks that are linked by non-covalent interactions.^[1] Notably, this field makes use of motifs featuring robust and reversible hydrogen bonds.^[2] For instance, in biological systems, hydrogen bonding is utilized to ensure the necessary reversibility in molecular associations. The iconic DNA double helix exemplifies this, where hydrogen bonds between Watson-Crick base pairs (adenine-thymine and guanine-cytosine) dictate its structure.^[3] Subsequently, it was discovered that DNA can also adopt alternative hydrogen-bonded configurations, such as guanine quadruplexes, whose structure comprise layers of four guanine molecules bound together by Hoogsteen-type hydrogen bonds.^[4]

By means of a quantum chemical study, we have previously demonstrated that the hydrogen bonds within guanine quartets contain a substantial synergistic effect, primarily attributed to the attractive orbital interactions.^[5] This Hoogsteen base pair comprises one guanine unit with two hydrogen-bond acceptors binding to another guanine unit with two hydrogen-bond donors. As a result, charge flows within the hydrogen bonds caused by the donor–acceptor interaction between the donating σ lone-pair-like orbitals on the oxygen and nitrogen atoms of one guanine base, and the accepting σ^* orbital on the N–H groups of another guanine base. Note that this electronic mechanism demonstrates the important covalent character of hydrogen bonds.^[5–6] Consequently, this induces charge separation within the dimer, making it better for subsequent hydrogen bonding compared to the original monomer. Later, González-Rodríguez *et al.* achieved the assembly of hydrogen-bonded quartets through the synthesis of a ditopic monomer based on guanosine and cytidine nucleosides at the termini and linked by a linear and rigid π -conjugated *p*-diethynylbenzene linker.^[7] Recently, these authors have shown that these quartets are able to stack and form tube-like nanostructures, revealing their similarity with guanine quartets.^[8]

Inspired by the work of González-Rodríguez *et al.*,^[7] we have recently designed a series of building blocks for self-assembled hydrogen-bonded macrocycles with rigid linear π -conjugated acetylene linkers connecting a hydrogen-bond acceptor to a hydrogen-bond donor, with all three hydrogen-bonds pointing in the same direction.^[9] This acetylene linker plays an unprecedented non-innocent role in the cooperativity of these hydrogen-bonded macrocycles by abstracting electron density from the hydrogen-bond acceptor and donor. As a result, the hydrogen-bond acceptor becomes less negatively charged, which hampers both the hydrogen bond strength and the cooperativity in these hydrogen-bonded macrocycles. This effect becomes more pronounced when the size of the acetylene linker increases.

[a] D. Almacellas, Prof. Dr. J. Poater
Departament de Química Inorgànica i Orgànica & IQTCUB, Universitat de Barcelona, Martí i Franquès 1–11, 08028 Barcelona (Spain)
E-mail: jordi.poater@ub.edu

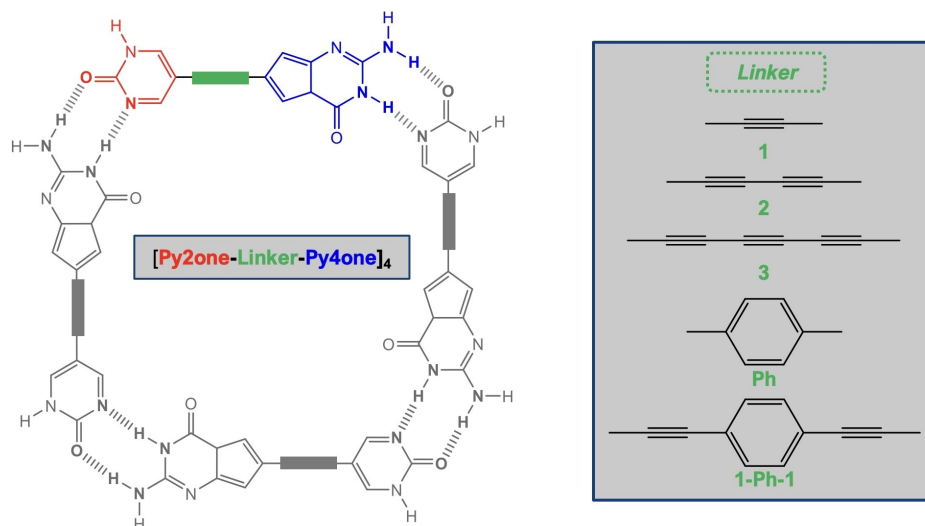
[b] Dr. S. C. C. van der Lubbe, A. A. Grosch, I. Tsagri, Dr. P. Vermeeren, Prof. Dr. C. Fonseca Guerra
Department of Chemistry and Pharmaceutical Sciences, AIMMS, Vrije Universiteit Amsterdam, De Boelelaan 1108, 1081 HZ Amsterdam (The Netherlands)
E-mail: p.vermeeren@vu.nl
c.fonseca Guerra@vu.nl
Homepage: <https://www.theochem.nl>

[c] Prof. Dr. J. Poater
ICREA, Passeig Lluís Companys 23, 08010 Barcelona (Spain)

Supporting information for this article is available on the WWW under <https://doi.org/10.1002/ejoc.202301164>

This article is part of the Special Collection Physical Organic Chemistry.

© 2023 The Authors. European Journal of Organic Chemistry published by Wiley-VCH GmbH. This is an open access article under the terms of the Creative Commons Attribution Non-Commercial NoDerivs License, which permits use and distribution in any medium, provided the original work is properly cited, the use is non-commercial and no modifications or adaptations are made.



Scheme 1. Schematic representation of quartet consisting of monomers with a hydrogen-bond acceptor side, pyrimidin-2(1H)-one (**Py2one**; red), and hydrogen-bond donor side, 2-amino-3,4a-dihydro-4H-cyclopenta[d]pyrimidin-4-one (**Py4one**; blue) with a linear π -conjugated linker (**Linker**; green).

In the present work, we propose a series of new supramolecular building blocks derived from the well-known guanine-cytosine base pair (Scheme 1). We have designed a series of monomers, referred to as **Py2one-Linker-Py4one**, formed by a hydrogen-bond acceptor side, consisting of pyrimidin-2(1H)-one (**Py2one**; red), and a hydrogen-bond donor side, consisting of 2-amino-3,4a-dihydro-4H-cyclopenta[d]pyrimidin-4-one (**Py4one**; blue), connected by a rigid linear π -conjugated linker (**Linker**; green). As can be seen, **Py2one** is derived from guanine, whereas **Py4one** is derived from cytosine (the latter lacks the amino group thus the third hydrogen bond as in guanine-cytosine pair cannot be formed). When four identical monomers are combined, they can form hydrogen-bonded quartets $[\text{Py2one-Linker-Py4one}]_4$, where their two hydrogen bonds point in the same direction. As earlier discussed,^[5,10] we know that in such a macrocycle, the hydrogen bonding can be strengthened by charge separation in the σ -electronic system through the covalent component in the hydrogen bonds and hence demonstrate cooperativity. Here, we want to investigate and understand the mechanism behind the synergy in the σ - and π -electronic systems of these macrocycles. This quantum chemical study performed with the Amsterdam Density Functional (ADF) program^[11] using ZORA-BLYP-D3(BJ)/TZ2P^[12] is based on a quantitative Kohn-Sham molecular orbital theory together with an energy decomposition analysis (EDA),^[13] complemented by a Voronoi deformation density (VDD) analysis^[14] of the charge distribution to monitor the electronic rearrangements and flow of the formed hydrogen bonds. The goal is to propose design principles for new supramolecular macrocycles.

Results and Discussion

Hydrogen-Bonded Quartets: Structure and Bond Strength

The equilibrium geometries of the $[\text{Py2one-Linker-Py4one}]_4$ quartets are enclosed in Figure 1, together with their hydrogen bond lengths and total bonding energies (Table 1). We find that introducing an acetylene linker hardly affects the hydrogen bonding energy with respect to the parent macrocycle, from $-75.4 \text{ kcal mol}^{-1}$ for **Py2one-Py4one** to $-74.5 \text{ kcal mol}^{-1}$ for **Py2one-1-Py4one**. Elongating the linker to two, three and four acetylene units makes the hydrogen bonds slightly stronger, namely, $-75.8 \text{ kcal mol}^{-1}$ for **Py2one-2-Py4one**, $-76.5 \text{ kcal mol}^{-1}$ for **Py2one-3-Py4one** and to $-76.7 \text{ kcal mol}^{-1}$ for **Py2one-4-Py4one**. For **Py2one-5-Py4one**, then complexation energy slightly decreases (*i.e.*, becomes weaker) to $-76.5 \text{ kcal mol}^{-1}$. These small changes in the hydrogen bond strength are also observed in the hydrogen bond lengths within the quartets (Figure 1). Where the outer hydrogen bond becomes slightly longer upon increasing the linker size, the opposite is observed for the inner hydrogen bond (denoted as

Table 1. Bonding and interaction energies (in kcal mol^{-1}) of the $[\text{Py2one-Linker-Py4one}]_4$ quartets with a different number of acetylene linkers.^[a,b]

| System | ΔE | ΔE_{strain} | ΔE_{int} | ΔE_{sum} | ΔE_{syn} |
|------------------------|------------|----------------------------|-------------------------|-------------------------|-------------------------|
| Py2one-Py4one | -75.4 | 7.3 | -82.7 | -75.9 | -6.8 |
| Py2one-1-Py4one | -74.5 | 7.2 | -81.7 | -77.4 | -4.3 |
| Py2one-2-Py4one | -75.8 | 7.0 | -82.8 | -79.5 | -3.3 |
| Py2one-3-Py4one | -76.5 | 6.9 | -83.4 | -80.6 | -2.8 |
| Py2one-4-Py4one | -76.7 | 6.7 | -83.4 | -81.0 | -2.4 |
| Py2one-5-Py4one | -76.5 | 7.0 | -83.5 | -81.4 | -2.1 |

[a] Computed at ZORA-BLYP-D3(BJ)/TZ2P. [b] Total complexation energy, *i.e.*, hydrogen bond energy, is computed as: $\Delta E = \Delta E_{\text{strain}} + \Delta E_{\text{int}}$; and synergy is computed as: $\Delta E_{\text{syn}} = \Delta E_{\text{int}} - \Delta E_{\text{sum}}$.

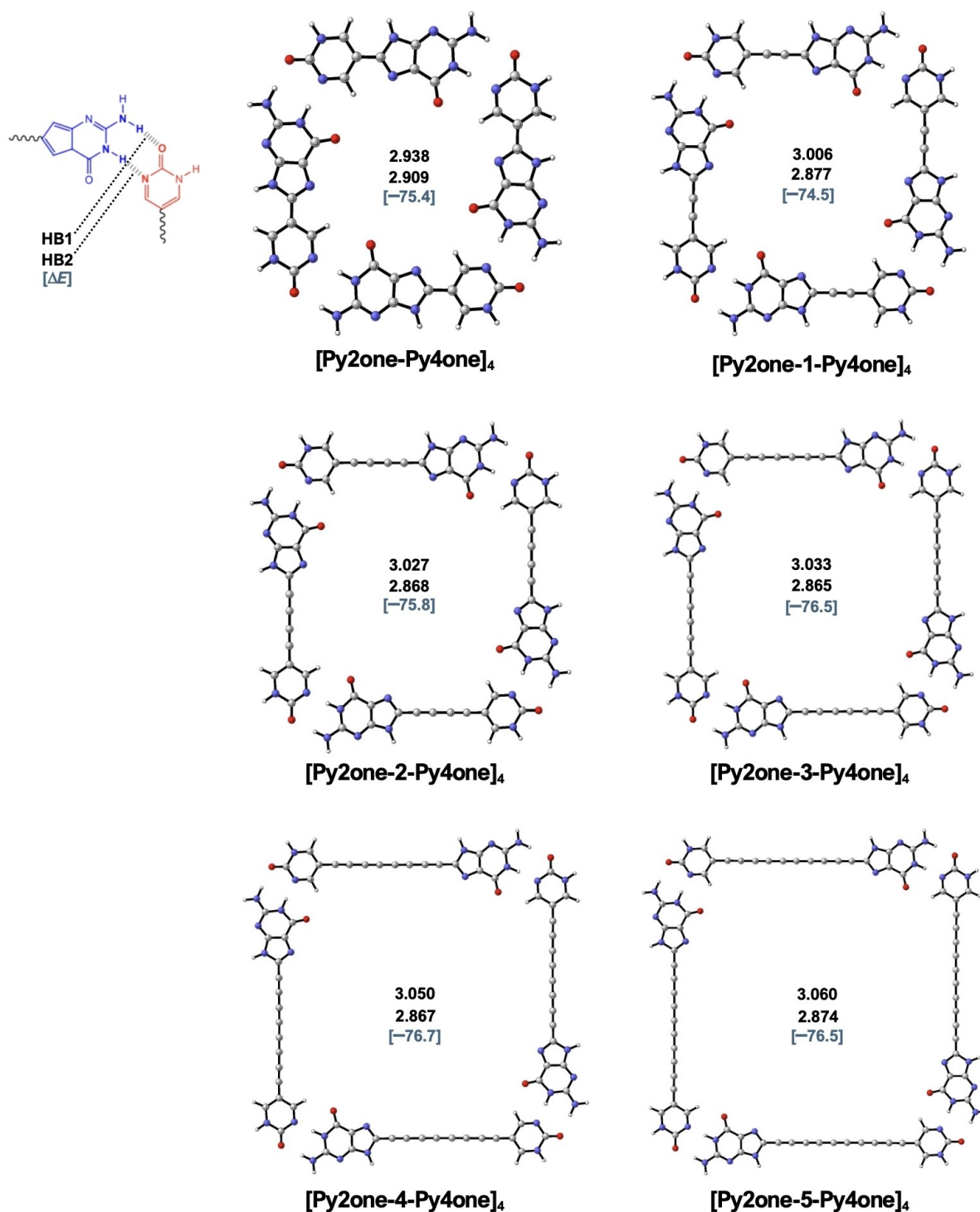


Figure 1. Geometries of [Py2one-Linker-Py4one]₄ quartets with a different number of acetylene linkers, including hydrogen bond lengths (in Å) and bonding energies (in brackets and kcal mol⁻¹). Computed at ZORA-BLYP-D3(BJ)/TZ2P.

HB1 and HB2 in Figure 1, respectively), except for the two longest linkers.

The activation strain model (ASM)^[15] is applied with the aim to better understand the hydrogen bond strengths of the quartets and shows that the interaction energy determines the trend in the hydrogen bond strengths (Table 1). Thus, in line with the hydrogen bond strength, the interaction energy

between the monomers that constitute the quartet slightly increases (*i.e.*, becomes stronger) from one to three acetylene units (from -81.7 to -83.5 kcal mol⁻¹ from **Py2one-1-Py4one** to **Py2one-5-Py4one**). On the other hand, the strain energy remains quite constant in all cases and originates from the N-H bond stretch as a result of the formation of the hydrogen bonds

between the interacting monomers, based on the fact that the geometry of the monomer is hardly affected by complexation.

To pinpoint the cooperative effect in the hydrogen bonds that constitute the [Py2one-Linker-Py4one]₄ macrocycles, we have calculated the synergy (ΔE_{syn} , Eq. 4 in Computational Details) for all studied systems by comparing the interaction energy of the quartets with the sum of the pairwise interaction (Table 1 and Figure 1). The negative ΔE_{syn} value proves that all hydrogen bonds between the Py2one-Py4one monomers in the quartet are effectively more stabilizing than the hydrogen bonds in the dimer. The largest synergy among the studied quartets is found for the parent [Py2one-Py4one]₄, i.e., this system has the most negative ΔE_{syn} . The synergy becomes consistently smaller with the introduction of the acetylene linker, i.e., from -6.8 to -4.3 to -3.3 to -2.8 to -2.4 to -2.1 kcal mol⁻¹ from [Py2one-Py4one]₄ to [Py2one-1-Py4one]₄ to [Py2one-2-Py4one]₄ to [Py2one-3-Py4one]₄ to [Py2one-4-Py4one]₄ to [Py2one-5-Py4one]₄, respectively. Thus, this shows that introducing an acetylene linker plays a role in the cooperativity of the hydrogen bonds within these quartets, whose reason will be discussed later. We want to emphasize here that we have previously shown that this cooperative effect persists under experimental conditions as it still exists in organic solvents, such as chloroform.^[7a,9,10g]

Hydrogen-Bonded Dimers: Nature of Hydrogen Bonding

To understand the bonding mechanism behind the cooperative hydrogen bonds of the studied quartets [Py2one-Linker-Py4one]₄, we first focus on the dimers [Py2one-Linker-Py4one]₂ (geometries taken from the quartet). By performing the energy decomposition analysis (EDA), we show that ΔE_{int} gradually increases from -19.1 kcal mol⁻¹ for [Py2one-Py4one]₂ to -20.4 kcal mol⁻¹ for [Py2one-5-Py4one]₂ when an acetylene linker is introduced (Table 2). This small increase of ΔE_{int} with the linker is in line with the more stabilizing interaction energy in the above-discussed quartets. This trend is due to the strengthening of the stabilizing electrostatic interactions that make the hydrogen bonds in the dimer stronger when the size of the linker increases, namely, ΔV_{elstat} increases from -25.9 kcal mol⁻¹ for [Py2one-Py4one]₂ to -26.9 kcal mol⁻¹ for [Py2one-3-Py4one]₂. However, ΔV_{elstat} slightly decreases for

both [Py2one-4-Py4one]₂ and [Py2one-5-Py4one]₂, as well as ΔE_{Pauli} in agreement with their longer HB2 bond length (Figure 1). The orbital and dispersion interactions, on the other hand, remain almost constant or even point in opposite directions and hence are not trend-determining.

Further insight can be gained by performing Voronoi deformation density (VDD) analyses.^[14] With the inclusion of the acetylene linker, the hydrogen-bond acceptor Py2one becomes positively charged, from -5 to $+97$ milli-electrons from Py2one-Py4one to Py2one-5-Py4one, respectively (Figure 2). At the same time, the hydrogen-bond donor Py4one becomes even more positively charged from $+5$ to $+101$ milli-electrons from Py2one-Py4one to Py2one-5-Py4one, respectively. A small increase of positive charge is also observed on the frontier atoms involved in the two hydrogen bonds (Figure S1). This means that the linker is accepting electronic density,^[16] which should translate into less attractive electrostatic interaction between hydrogen-donor and -acceptor moieties between the monomers in the dimer when going from one to five acetylene linkers. Nevertheless, this is not happening in practice (Table 2), because upon increasing the size of the linker (i) the inner hydrogen bond distance decreases and (ii) the monomer with a linker contains more atoms. These two stabilizing effects eclipse the previously discussed increased positive charge on the termini of the monomers, making the ΔV_{elstat} slightly more stabilizing along the series of studied systems.

Additionally, by inspecting the studied macrocycles (Figure 1), one might expect an unconventional O...H-C hydrogen bond between the monomers to be present in these systems. However, this bond does not play a determinant role in the interaction. The O...H-C hydrogen bond becomes shorter from 2.848 Å to 2.683 Å to 2.640 Å to 2.630 Å to 2.620 Å and 2.622 Å from Py2one-Py4one to Py2one-1-Py4one to Py2one-2-Py4one to Py2one-3-Py4one to Py2one-4-Py4one and to Py2one-5-Py4one, respectively. By means of an EDA analysis in which the unoccupied orbitals of the two hydrogen-bond donors are removed and hence only the proposed O...H-C hydrogen bond could engage in a donor-acceptor interaction, we found that it is not a hydrogen bond with any covalent component. Our analysis reveals that there is hardly any charge transfer from Py4one to Py2one (only -5 – -7 milli-electrons, Table S1).

Table 2. Energy decomposition analysis of the hydrogen bond in the [Py2one-Linker-Py4one]₂ dimers with a different number of acetylene linkers (in kcal mol⁻¹).^[a,b,c]

| | ΔE_{int} | ΔV_{elstat} | ΔE_{Pauli} | ΔE_{σ} | ΔE_{π} | ΔE_{oi} | ΔE_{disp} |
|-----------------|-------------------------|----------------------------|---------------------------|---------------------|------------------|------------------------|--------------------------|
| Py2one-Py4one | -19.1 | -25.9 | 27.3 | -13.3 | -2.2 | -15.5 | -5.0 |
| Py2one-1-Py4one | -19.6 | -26.4 | 27.5 | -13.4 | -2.2 | -15.6 | -5.1 |
| Py2one-2-Py4one | -20.0 | -26.8 | 27.6 | -13.5 | -2.2 | -15.7 | -5.1 |
| Py2one-3-Py4one | -20.3 | -26.9 | 27.6 | -13.6 | -2.3 | -15.9 | -5.1 |
| Py2one-4-Py4one | -20.3 | -26.7 | 27.1 | -13.4 | -2.3 | -15.7 | -5.1 |
| Py2one-5-Py4one | -20.4 | -26.3 | 26.5 | -13.2 | -2.3 | -15.5 | -5.1 |

[a] Computed at ZORA-BLYP-D3(BJ)/TZ2P. [b] Geometries of dimers taken from the optimized quartets. [c] Interaction energy is decomposed as: $\Delta E_{\text{int}} = \Delta V_{\text{elstat}} + \Delta E_{\text{Pauli}} + \Delta E_{\text{oi}} + \Delta E_{\text{disp}}$.

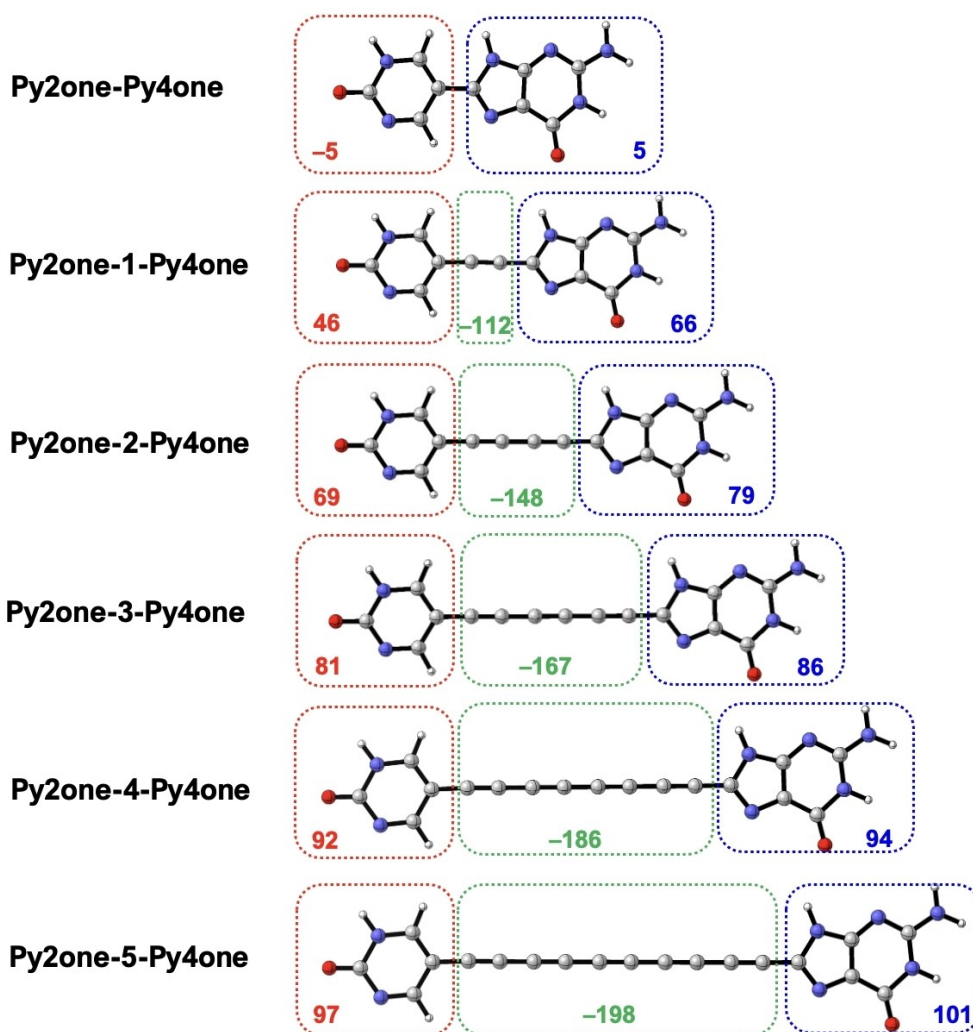


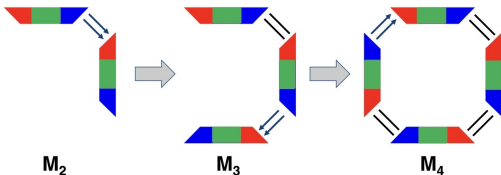
Figure 2. Voronoi deformation density (VDD) charges Q (in milli-electrons) for the **Py2one-Linker-Py4one** monomers in the geometry of the optimized quartet, where the total VDD charge on the hydrogen-bond acceptor (**Py2one**; red), linker (**Linker**; green), and hydrogen-bond donor (**Py4one**; blue) are given. Computed at ZORA-BLYP-D3(BJ)/TZ2P. Check Figure S1 for the charges of the frontier atoms.

Hydrogen-Bonded Quartets: Cooperativity

Next, we can proceed to analyze the origin of the synergy in the **[Py2one-Linker-Py4one]₄** quartets by stepwise adding a monomer to the system, *i.e.*, $M_2 = \text{monomer} + \text{monomer}$; $M_3 = \text{dimer} + \text{monomer}$; and $M_4 = \text{trimer} + \text{monomer}$. As mentioned above, all quartets show cooperativity ($\Delta E_{\text{syn}} < 0$), however, the ΔE_{syn} becomes smaller when elongating the acetylene linker, *i.e.*, from -6.8 to -2.1 kcal mol⁻¹ from **[Py2one-Py4one]₄** to **[Py2one-5-Py4one]₄**, respectively. By performing the energy decomposition analysis, we find that the electrostatic and orbital interactions are the two main contributors to the synergy (Table 3). Both ΔV_{elstat} and ΔE_{oi} become more stable upon stepwise formation of the quartets. For instance, for **[Py2one-Py4one]₄**, ΔV_{elstat} increases from -25.9 to -26.2 to -53.6 kcal mol⁻¹ from M_2 to M_3 to M_4 , whereas ΔE_{oi} increases from -15.5 to -16.2 to -34.2 kcal mol⁻¹ from M_2 to M_3 to M_4 , respectively. In line with ΔE_{syn} , both ΔV_{elstat} and ΔE_{oi} become weaker with a longer acetylene linker, *i.e.*, ΔV_{elstat} decreases

from -3.0 to -0.8 kcal mol⁻¹ and ΔE_{oi} decreases from -3.7 to -1.3 kcal mol⁻¹ from **[Py2one-Py4one]₄** to **[Py2one-5-Py4one]₄**. Noteworthy, even though the σ -orbital interaction is the strongest in the interaction energy of the hydrogen bonds, both σ - and π -orbital interactions contribute equally to the synergy in these macrocycles and decrease similarly along the studied systems.

The decisive role of both electrostatic and orbital interactions in the synergy of these macrocycles originates from the charge transfer between the occupied and unoccupied orbitals of the interacting monomers, giving rise to the charge separation in the systems. This charge separation decreases with a longer acetylene linker. The charge transfer between the monomers that constitute the quartet can be quantified by means of the Voronoi deformation density (VDD) charge analysis (Figure 3). Upon the stepwise formation of the quartet, the σ -donor-acceptor interactions between the hydrogen-bond donor and hydrogen-bond acceptor lead to a charge transfer between the interacting fragments. As a result, the charge flows

Table 3. Energy decomposition analysis and synergy (in kcal mol⁻¹) of the stepwise formation of the [Py2One-Linker-Py4One]₄ quartets with a different number of acetylene linkers.^[a,b]


| System | | ΔE_{int} | ΔV_{elstat} | ΔE_{Pauli} | ΔE_{σ} | ΔE_{π} | ΔE_{oi} | ΔE_{disp} |
|-----------------|-------------------------|-------------------------|----------------------------|---------------------------|---------------------|------------------|------------------------|--------------------------|
| Py2one-Py4one | M ₂ | -19.2 | -25.9 | 27.2 | -13.3 | -2.2 | -15.5 | -5.0 |
| | M ₃ | -20.3 | -26.2 | 27.1 | -13.7 | -2.5 | -16.2 | -5.0 |
| | M ₄ | -43.2 | -53.6 | 54.6 | -28.2 | -6.0 | -34.2 | -10.0 |
| | ΔE_{syn} | -6.8 | -3.0 | -0.1 | -1.9 | -1.8 | -3.7 | 0.0 |
| Py2one-1-Py4one | M ₂ | -19.6 | -26.4 | 27.5 | -13.4 | -2.2 | -15.6 | -5.1 |
| | M ₃ | -20.2 | -26.7 | 27.6 | -13.6 | -2.4 | -16.0 | -5.1 |
| | M ₄ | -42.0 | -53.7 | 54.9 | -27.7 | -5.3 | -33.0 | -10.2 |
| | ΔE_{syn} | -4.3 | -1.6 | -0.1 | -1.3 | -1.3 | -2.6 | 0.0 |
| Py2one-2-Py4one | M ₂ | -20.0 | -26.8 | 27.6 | -13.5 | -2.2 | -15.7 | -5.1 |
| | M ₃ | -20.5 | -26.9 | 27.6 | -13.7 | -2.4 | -16.1 | -5.1 |
| | M ₄ | -42.3 | -54.3 | 55.3 | -27.8 | -5.3 | -33.1 | -10.2 |
| | ΔE_{syn} | -3.3 | -1.3 | -0.1 | -0.9 | -1.0 | -1.9 | 0.0 |
| Py2one-3-Py4one | M ₂ | -20.2 | -26.9 | 27.7 | -13.6 | -2.3 | -15.9 | -5.1 |
| | M ₃ | -20.7 | -27.0 | 27.5 | -13.7 | -2.4 | -16.1 | -5.1 |
| | M ₄ | -42.3 | -54.4 | 55.3 | -27.8 | -5.2 | -33.0 | -10.2 |
| | ΔE_{syn} | -2.8 | -1.1 | 0.0 | -0.8 | -0.9 | -1.7 | 0.0 |
| Py2one-4-Py4one | M ₂ | -20.3 | -26.7 | 27.1 | -13.4 | -2.3 | -15.7 | -5.1 |
| | M ₃ | -20.7 | -26.7 | 27.0 | -13.5 | -2.4 | -15.9 | -5.1 |
| | M ₄ | -42.4 | -53.9 | 54.2 | -27.4 | -5.2 | -32.5 | -10.2 |
| | ΔE_{syn} | -2.4 | -0.9 | -0.1 | -0.7 | -0.7 | -1.4 | 0.0 |
| Py2one-5-Py4one | M ₂ | -20.4 | -26.3 | 26.5 | -13.2 | -2.3 | -15.5 | -5.1 |
| | M ₃ | -20.8 | -26.4 | 26.4 | -13.3 | -2.4 | -15.7 | -5.1 |
| | M ₄ | -42.4 | -53.2 | 52.9 | -26.9 | -5.1 | -32.0 | -10.1 |
| | ΔE_{syn} | -2.1 | -0.8 | 0.0 | -0.6 | -0.6 | -1.3 | 0.0 |

[a] Computed at ZORA-BLYP-D3(BJ)/TZ2P. [b] M₂ = monomer + monomer, M₃ = dimer + monomer, M₄ = trimer + monomer.

from one terminal monomer to the other terminal monomer resulting in charge separation in the system, which systematically increases upon stepwise formation of the quartet. The charge transfer between the fragments, however, reduces when the acetylene linker is introduced, and elongated, due to the electron acceptance capability of the linker. For instance, in case of **Py2one-Py4one**, the charge of the hydrogen-bond acceptor monomer increases from -178 to -188 milli-electrons from M₂ to M₃, whereas for **Py2one-1-Py4one**, the charge of the hydrogen-bond acceptor is reduced to -169 and -173 milli-electrons from M₂ to M₃ (Figure 3). Thus, for these systems, constructing the quartet is accompanied by less charge separation.

As a consequence of the charge separation in the system, the hydrogen-bond acceptor becomes more negatively charged

(red rectangle in Figure 4) and the hydrogen-bond donor more positively charged (blue rectangle in Figure 4) compared to their respective monomers. This effect is most prominent when the dimer M₂ is formed and only small for the trimer M₃. For instance, in the case of **Py2one-Py4one**, the hydrogen-bond acceptor **Py2one** becomes more negatively charged from -5 to -38 to -49 milli-electrons from M to M₂ and M₃, respectively, whereas the hydrogen-bond acceptor **Py4one** becomes more positively charged from +5 to +55 to +63 milli-electrons. The introduction of the acetylene linker, again, causes a decrease in this charge separation. Furthermore, in line with what we have already pointed out above for the dimers (Table 2), the increase of ΔV_{elstat} with the longer acetylene linker is due to shorter hydrogen bond distance in the quartet and together with having more atoms this translates into slightly larger sum of the

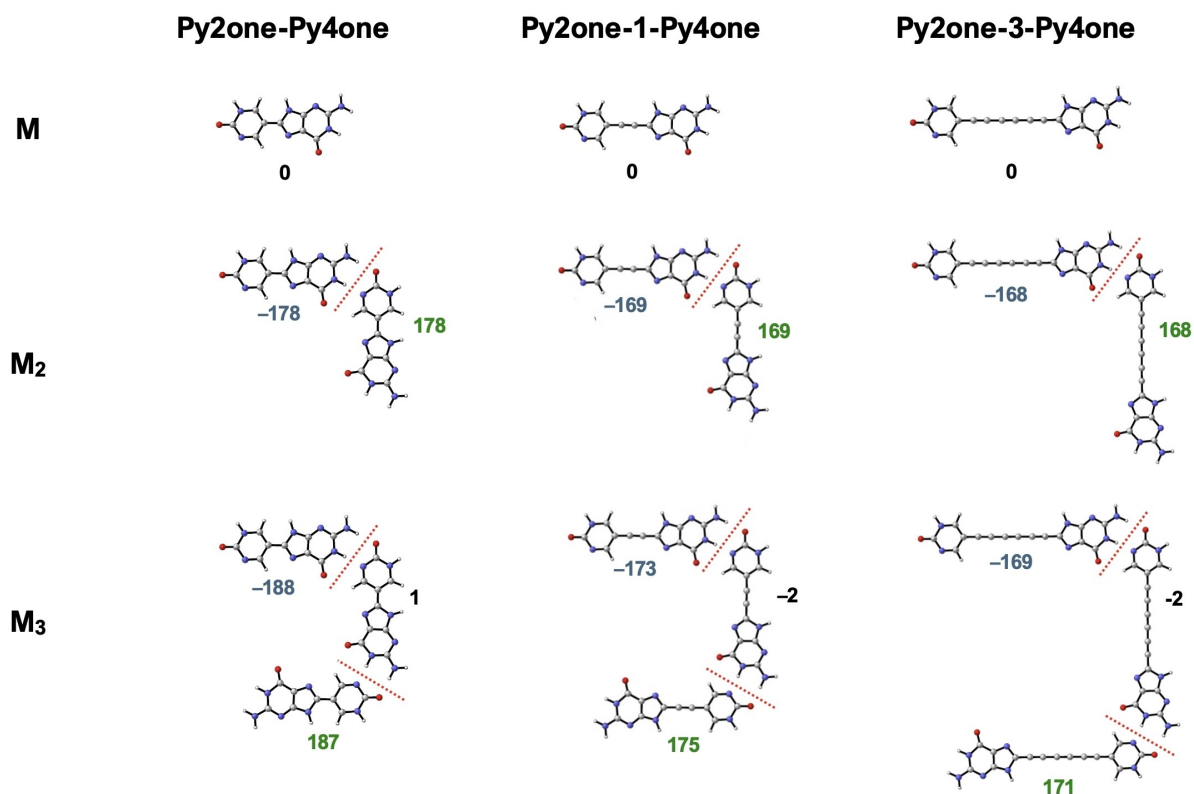


Figure 3. VDD charges Q (in milli-electrons) monomers upon stepwise formation of the $[\text{Py2one-Py4one}]_4$, $[\text{Py2one-1-Py4one}]_4$, and $[\text{Py2one-3-Py4one}]_4$ quartets, computed at ZORA-BLYP-D3(BJ)/TZ2P. VDD data for $[\text{Py2one-4-Py4one}]_4$ and $[\text{Py2one-5-Py4one}]_4$ quartets is enclosed in Figure S2.

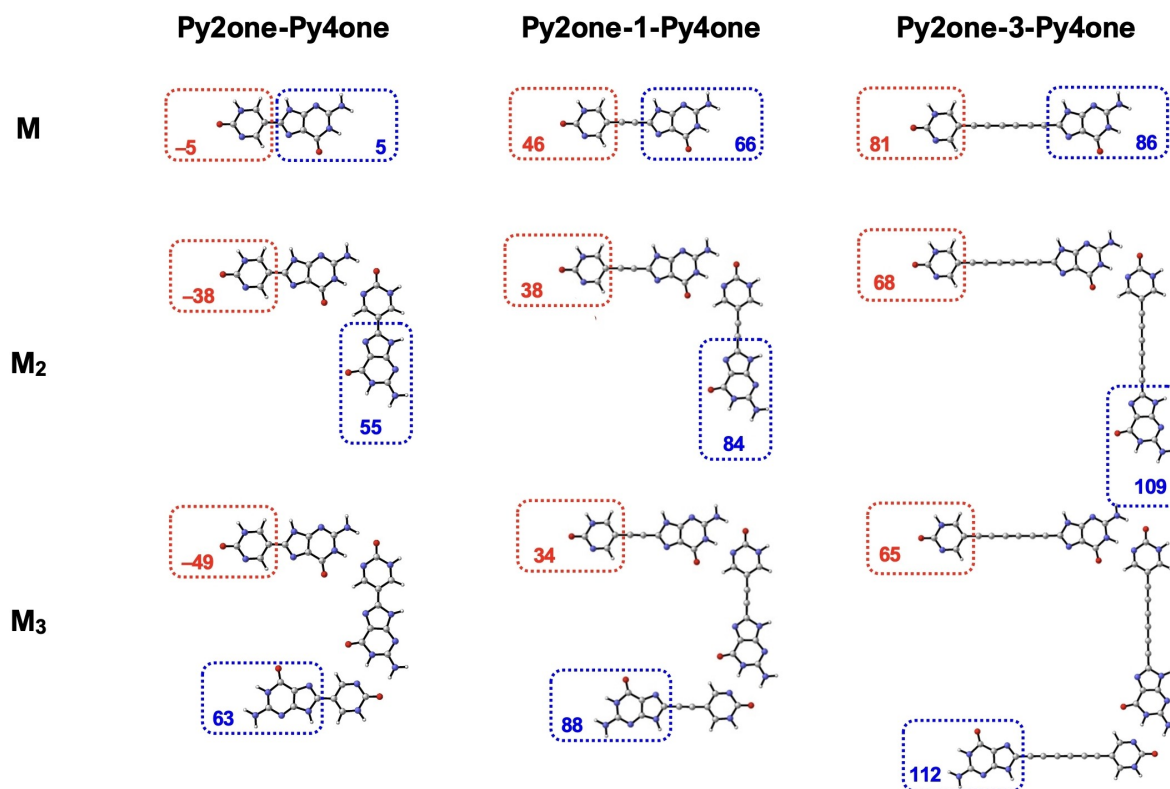


Figure 4. VDD charges Q (in milli-electrons) of the terminal hydrogen-bond acceptor (Py2one; red) and hydrogen-bond donor (Py4one; blue) for fragments upon stepwise formation of the $[\text{Py2one-Py4one}]_4$, $[\text{Py2one-1-Py4one}]_4$, and $[\text{Py2one-3-Py4one}]_4$ quartets, computed at ZORA-BLYP-D3(BJ)/TZ2P. VDD data for $[\text{Py2one-4-Py4one}]_4$ and $[\text{Py2one-5-Py4one}]_4$ quartets is enclosed in Figure S3.

pairwise interactions (ΔE_{sum} in Table S2), from -99.5 to -106.1 kcal mol $^{-1}$ from **Py2one-Py4one** to **Py2one-3-Py4one**, and thus smaller synergy when the linker increases.

The charge transfer upon stepwise formation of the **[Py2one-Linker-Py4one] $_4$** quartet also causes synergy in the σ -orbital interactions, which has been quantified by means of a Kohn-Sham molecular orbital analysis. The accumulation of charge on the terminal hydrogen bond acceptor (**Py2one**) and hydrogen bond donor (**Py4one**) has a direct effect on the orbital energies of the orbitals involved in the hydrogen bond between the monomers. The increased negative charge on **Py2one** destabilizes the σ -HOMO orbitals (Table S3 and Figure S4), whereas the more positive charge on **Py4one** stabilizes the σ -LUMO orbitals. For example, in the case of **[Py2one-Py4one] $_4$** , the orbital energies of σ -HOMOs are destabilized from -5.95 and -6.26 eV in **M** to -5.37 and -5.78 eV in **M $_3$** . On the other hand, the σ -LUMOs are stabilized from -1.37 and -0.20 eV for **M** to -1.38 and -0.23 eV for **M $_3$** . The σ -HOMO-LUMO gap between the interacting fragments, therefore, becomes smaller, leading to the observed enhanced σ -orbital interactions as shown in Table 3.

Furthermore, the π -orbital interactions are also affected by the charge separation. The more negative charge on **Py2one** not only destabilizes the σ -HOMO orbitals and the more positive charge on **Py4one** not only stabilizes the σ -LUMO orbitals, but also the π -HOMO and π -LUMO orbitals of the monomers. Consequently, π -polarization is also enhanced due to the reduction of the π -HOMO-LUMO gap (Table S4). Note that, as established by the reduced charge transfer, the effect on the orbital energies becomes less pronounced when the acetylene linker increases. This, ultimately, leads to less synergy in both the σ - and π -orbital interaction when the linker becomes longer.

Hydrogen-Bonded Quartets: Expanding towards Phenyl Linkers

In the final section of this manuscript, we aim to systematically modify our above-studied model monomers to compare with the monomer synthesized by González-Rodríguez *et al.*^[7] For such an aim, we first introduce a phenyl linker (**Py2one-Ph-Py4one**) and an acetylene-phenyl-acetylene linker (**Py2one-1-Ph-1-Py4one**) between the hydrogen-bond donor and acceptor units. Both new quartets result in a strengthening of the hydrogen bonds, from -76.9 to -83.1 to -78.6 kcal mol $^{-1}$ from **[Py2one-Py4one] $_4$** to **[Py2one-Ph-Py4one] $_4$** to **[Py2one-1-Ph-1-Py4one] $_4$** , respectively (Figure 5). Furthermore, they are also stabilized by cooperativity, originating from more attractive electrostatic and orbital interactions upon building the quartet (Table S5). Nonetheless, the computed synergy for both systems is smaller than for the parent system, namely, ΔE_{syn} decreases from -6.8 kcal mol $^{-1}$ in **[Py2one-Py4one] $_4$** to -2.8 and -1.5 kcal mol $^{-1}$ for **[Py2one-Ph-Py4one] $_4$** and **[Py2one-1-Ph-1-Py4one] $_4$** , respectively. This weakening of the cooperativity in the case of **[Py2one-Ph-Py4one] $_4$** is a result of the electron-donating capability of the phenyl linker, making both hydrogen-donor and -acceptor terminal groups negatively charged (Figure S5), and thus hampering the cooperativity. At difference, when two acetylene units are added next to the phenyl linker, the electron-donating character of the phenyl linker is counterbalanced, making the **[Py2one-1-Ph-1-Py4one] $_4$** quartet act similar to the original acetylene linkers earlier discussed.

At last, we examine the hydrogen-bonded quartet synthesized by González-Rodríguez *et al.*^[7] that consists of an acetylene-phenyl-acetylene linker that connects a cytosine to a guanine nucleobase (**C-1-Ph-1-G**). In contrast to our earlier studied monomers, the cytosine-based terminus now has two

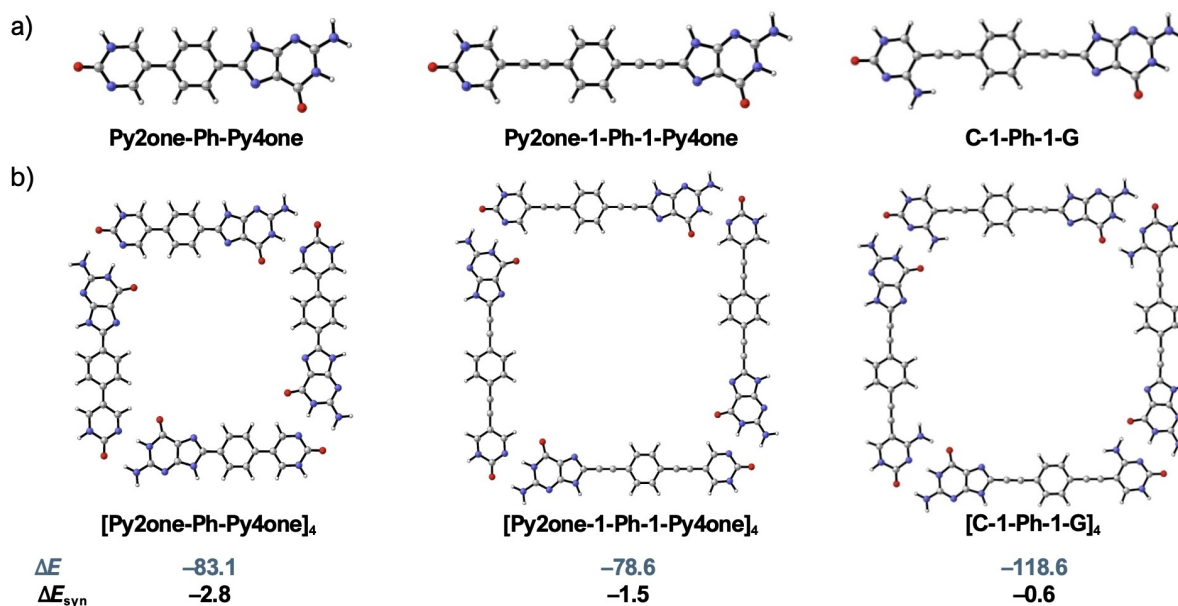


Figure 5. Geometries of a) monomers with phenyl linker (**Py2one-Ph-Py4one**), acetylene-phenyl-acetylene linker (**Py2one-1-Ph-1-Py4one**), as well as the simplified monomer synthesized by González-Rodríguez *et al.*, constituted of cytosine and guanine nucleobases connected via an acetylene and phenyl linker (**C-1-Ph-1-G**); and b) their respective quartets with hydrogen bonding energy and synergy (in kcal mol $^{-1}$). Computed at ZORA-BLYP-D3(BJ)/TZ2P.

hydrogen-bond acceptors and one hydrogen-bond donor, whereas the guanine-based terminus has the opposite, namely, one hydrogen-bond acceptor and two hydrogen-bond donors. Resultingly, the cooperativity in the quartets constructed from these monomers is significantly smaller than the cooperativity in [Py2one-Py4one]₄, namely $-0.6 \text{ kcal mol}^{-1}$ (Figure 5). This is due to the fact that not all hydrogen bonds formed point in the same direction, which is one of the basic forms to strengthen cooperativity, as we have shown in our previous study on the cooperativity of guanine and xanthine quartets.^[5a,10f]

Conclusions

In this work, we have quantum chemically analyzed the cooperativity in a series of hydrogen-bonded quartets constructed from building blocks that consist of a hydrogen-bond donor side and a hydrogen-bond acceptor side connected with linear, rigid π -conjugated linkers of different lengths. All macrocycles show a cooperative effect, its magnitude, however, decreases, *i.e.*, becomes less stabilizing, upon increasing the size of the acetylene linker. This emerges from our dispersion-corrected density functional theory (DFT-D) calculations based on quantitative Kohn-Sham molecular orbital theory and energy decomposition analyses.

The cooperativity in these macrocyclic structures arises from the charge transfer from the occupied σ -orbitals of the hydrogen-bond acceptors to the unoccupied σ -orbitals of the hydrogen-bond donors, leading to an increased charge separation in the system. This separation causes the hydrogen-bond acceptor to become more negatively charged whereas the hydrogen-bond donor becomes more positively charged. This charge transfer is decreased when a longer acetylene linker is introduced due to the linker's ability to abstract electron density from both the terminal hydrogen-bond donor and acceptor groups.

Finally, the above conclusions are extended towards the previously synthesized hydrogen-bonded macrocycles based on guanosine and cytidine nucleosides,^[7] with the aim to establish design principles for the design of related strengthened cooperative macrocycles for different applications in supramolecular chemistry.

Computational Details

The quartets and monomers have been optimized in planar symmetry (C_s). For the monomers optimizations without any symmetry constraints (C_1) have also been performed and were verified to be true minima (zero imaginary frequencies). The difference in energy between C_s and C_1 optimizations for selected monomers and quartets is only a few tenths of a kcal mol^{-1} , except for Py2one-Ph-Py4one (Tables S6–S9).

The hydrogen bond energy ΔE of the quartet is defined as [Eq. (1)]:

$$\Delta E = E_{\text{quartet}} - 4 E_{\text{monomer}} \quad (1)$$

where E_{quartet} is the energy of the optimized quartet in C_s symmetry, and E_{monomer} is the energy of the C_1 optimized monomer. This ΔE can be divided into two components by means of the activation strain model (ASM)^[15] [Eq. (2)]:

$$\Delta E = \Delta E_{\text{strain}} + \Delta E_{\text{int}} \quad (2)$$

In this formula, the strain energy ΔE_{strain} is the amount of energy required to deform the individual monomers from their equilibrium structure to the geometry that they acquire in the quartet. The interaction energy ΔE_{int} corresponds to the actual energy change when the prepared monomers are combined to form the quartet.

The cooperativity in the hydrogen bonds (HBs) in the quartets is quantified by comparing the interaction energy of the quartet (ΔE_{int}) with the sum of the individual pairwise interactions for all possible pairs of monomers (ΔE_{sum}) in the quartet (Scheme 2), defined as [Eq. (3)]:

$$\Delta E_{\text{sum}} = 4 \Delta E_{\text{pair}} + 2 \Delta E_{\text{diag}} \quad (3)$$

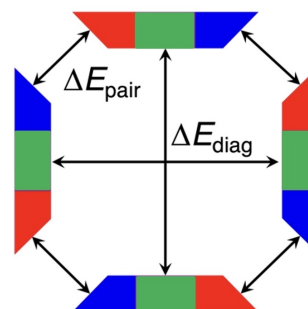
Here, ΔE_{pair} is the interaction between two neighboring monomers (*i.e.*, the interaction between two hydrogen-bonded monomers in the geometry of the quartet) and ΔE_{diag} is the interaction between two mutually diagonally oriented monomers (*i.e.*, the interaction between two non-hydrogen bonded monomers in the geometry of the quartet). The synergy occurring in the quartet is then defined as the difference [Eq. (4)]:

$$\Delta E_{\text{syn}} = \Delta E_{\text{int}} - \Delta E_{\text{sum}} \quad (4)$$

Thus, a negative value of ΔE_{syn} corresponds to a stabilizing cooperative effect, meaning that the quartet stability is reinforced due to the occurrence of all hydrogen bonds simultaneously.

Supporting Information

The Supporting Information encloses an extended description of the computational details; complementary EDA analyses on some of the dimers, together with their σ and π orbital energies; EDA data of systems [Py2One-Phe-Py4One]₄, [Py2One-1-Phe-1-Py4One]₄, [C-1-Ph-1-G]₄; and Cartesian coordinates and electronic energies of all systems under analysis.



Scheme 2. Pair and diagonal interactions in the quartet.

Acknowledgements

D.A. is grateful to the Ministerio de Ciencia e Innovación for the PRE2018-084044 fellowship. J.P. thanks the Spanish MINECO (PID2019-106830GB-I00, PID2022-138861NB-I00, and CEX2021-001202-M) and the Generalitat de Catalunya (2021SGR442). P.V. and C.F.G. acknowledge the financial support from the Netherlands Organization for Scientific Research (NWO).

Conflict of Interests

There are no conflicts to declare.

Data Availability Statement

The data that support the findings of this study are available in the supplementary material of this article.

Keywords: Cooperativity · Density Functional Theory · Energy Decomposition Analysis · Hydrogen Bonds · Self-Assembly

- [1] a) R. Chakrabarty, P. S. Mukherjee, P. J. Stang, *Chem. Rev.* **2011**, *111*, 6810–6918; b) A. del Prado, D. González-Rodríguez, Y. L. Wu, *ChemistryOpen* **2020**, *9*, 409–430; c) G. R. Desiraju, *Angew. Chem. Int. Ed.* **1995**, *34*, 2311–2327; d) J. M. Lehn, *Supramolecular Chemistry*, VCH, Weinheim, **1995**.
- [2] a) W. P. J. Appel, M. M. L. Nieuwenhuizen, M. Lutz, B. F. M. de Waal, A. R. A. Palmans, E. W. Meijer, *Chem. Sci.* **2014**, *5*, 3735–3745; b) F. H. Beijer, R. P. Sijbesma, H. Kooijman, A. L. Spek, E. W. Meijer, *J. Am. Chem. Soc.* **1998**, *120*, 6761–6769; c) H. M. Coubrough, S. C. C. van der Lubbe, K. Hetherington, A. Minard, C. Pask, M. J. Howard, C. Fonseca Guerra, A. J. Wilson, *Chem. Eur. J.* **2019**, *25*, 785–795; d) S. H. M. Söntjens, R. P. Sijbesma, M. H. P. van Genderen, E. W. Meijer, *J. Am. Chem. Soc.* **2000**, *122*, 7487–7493.
- [3] a) J. M. Berg, J. L. Tymoczko, L. Stryer, *Biochemistry*, 5th Edition ed., W. H. Freeman and Company, New York, **2002**; b) W. Saenger, *Principles of Nucleic Acid Structure*, Springer, New York, **1984**; c) C. Fonseca Guerra, F. M. Bickelhaupt, *Angew. Chem. Int. Ed.* **1999**, *38*, 2942–2945; d) C. Fonseca Guerra, F. M. Bickelhaupt, *Angew. Chem. Int. Ed.* **2002**, *41*, 2092–2095; e) C. Fonseca Guerra, F. M. Bickelhaupt, J. G. Snijders, E. J. Baerends, *Chem. Eur. J.* **1999**, *5*, 3581–3594; f) C. Nieuwland, T. A. Hamlin, C. Fonseca Guerra, G. Barone, F. M. Bickelhaupt, *ChemistryOpen* **2022**, *11*, e202100231; g) C. Nieuwland, F. Zaccaria, C. Fonseca Guerra, *Phys. Chem. Chem. Phys.* **2020**, *22*, 21108–21118.
- [4] a) M. L. Bochman, K. Paeschke, V. A. Zakian, *Nat. Rev. Genet.* **2012**, *13*, 770–780; b) J. T. Davis, *Angew. Chem. Int. Ed.* **2004**, *43*, 668–698; c) L. Stefan, D. Monchaud, *Nat. Chem. Rev.* **2019**, *3*, 650–668; d) C. Nieuwland, C. Fonseca Guerra, in *Modern Avenues in Metal-Nucleic Acid Chemistry. Metal Ions in Life Sciences*, Vol. 25 (Eds.: J. Müller, B. Lippert, A. Sigel, H. Sigel, E. Freisinger, R. K. O. Sigel), CRC Press, Boca Raton, **2023**, pp. 343–372; e) I. O. de Luzuriaga, A. Sánchez-González, W. Synoradzki, X. Lopez, A. Gil, *Phys. Chem. Chem. Phys.* **2022**, *24*, 25918–25929; f) A. Sánchez-González, N. A. G. Bandeira, I. O. de Luzuriaga, F. F. Martins, S. Elleuchi, K. Jarraya, J. Lanuza, X. Lopez, M. J. Calhorda, A. Gil, *Molecules* **2021**, *26*, 4737.
- [5] a) C. Fonseca Guerra, H. Zijlstra, G. Paragi, F. M. Bickelhaupt, *Chem. Eur. J.* **2011**, *17*, 12612–12622; b) G. Paragi, C. Fonseca Guerra, *Chem. Eur. J.* **2017**, *23*, 3042–3050; c) F. Zaccaria, S. C. C. van der Lubbe, C. Nieuwland, T. A. Hamlin, C. Fonseca Guerra, *ChemPhysChem* **2021**, *22*, 2286–2296.
- [6] a) K. Morokuma, *Acc. Chem. Res.* **1977**, *10*, 294–300; b) H. Uemeyama, K. Morokuma, *J. Am. Chem. Soc.* **1977**, *99*, 1316–1332; c) S. C. C. van der Lubbe, C. Fonseca Guerra, *Chem. Asian J.* **2019**, *14*, 2760–2769; d) S. Yamabe, K. Morokuma, *J. Am. Chem. Soc.* **1975**, *97*, 4458–4465.
- [7] a) C. Montoro-García, N. Bilbao, I. M. Tsagri, F. Zaccaria, M. J. Mayoral, C. Fonseca Guerra, D. González-Rodríguez, *Chem. Eur. J.* **2018**, *24*, 11983–11991; b) C. Montoro-García, M. J. Mayoral, R. Chamorro, D. González-Rodríguez, *Angew. Chem. Int. Ed.* **2017**, *56*, 15649–15653; c) D. Serrano-Molina, C. Montoro-García, M. J. Mayoral, A. de Juan, D. González-Rodríguez, *J. Am. Chem. Soc.* **2022**, *144*, 5450–5460.
- [8] a) M. González-Sánchez, M. J. Mayoral, V. Vázquez-González, M. Paloncyova, I. Sancho-Casado, F. Aparicio, A. de Juan, G. Longhi, P. Norman, M. Linares, D. González-Rodríguez, *J. Am. Chem. Soc.* **2023**, *145*, 17805–17818; b) M. J. Mayoral, N. Bilbao, D. González-Rodríguez, *ChemistryOpen* **2016**, *5*, 10–32.
- [9] D. Almacellas, S. C. C. van der Lubbe, A. A. Grosch, I. Tsagri, P. Vermeeren, J. Poater, C. Fonseca Guerra, *ChemistryEurope* **2024**, *2*, e202300036.
- [10] a) L. de Azevedo Santos, D. Cesario, P. Vermeeren, S. C. C. van der Lubbe, F. Nunzi, C. Fonseca Guerra, *ChemPlusChem* **2022**, *87*, e202100436; b) J. Dominikowska, F. M. Bickelhaupt, M. Palusiak, C. Fonseca Guerra, *ChemPhysChem* **2016**, *17*, 474–480; c) A. N. Petelski, C. Fonseca Guerra, *ChemistryOpen* **2019**, *8*, 135–142; d) A. N. Petelski, C. Fonseca Guerra, *Chem. Asian J.* **2022**, *17*, e202201010; e) P. Vermeeren, L. P. Wolters, G. Paragi, C. Fonseca Guerra, *ChemPlusChem* **2021**, *86*, 812–819; f) L. P. Wolters, N. W. G. Smits, C. Fonseca Guerra, *Phys. Chem. Chem. Phys.* **2015**, *17*, 1585–1592; g) D. Almacellas, C. Fonseca Guerra, J. Poater, *Org. Biomol. Chem.* **2023**, *21*, 8403–8412.
- [11] G. te Velde, F. M. Bickelhaupt, E. J. Baerends, C. Fonseca Guerra, S. J. A. van Gisbergen, J. G. Snijders, T. Ziegler, *J. Comput. Chem.* **2001**, *22*, 931–967.
- [12] a) A. D. Becke, *Phys. Rev. A* **1988**, *38*, 3098–3100; b) S. Grimme, J. Antony, S. Ehrlich, H. Krieg, *J. Chem. Phys.* **2010**, *132*, 154104; c) S. Grimme, S. Ehrlich, L. Goerigk, *J. Comput. Chem.* **2011**, *32*, 1456–1465; d) C. T. Lee, W. T. Yang, R. G. Parr, *Phys. Rev. B* **1988**, *37*, 785–789; e) E. van Lenthe, E. J. Baerends, *J. Comput. Chem.* **2003**, *24*, 1142–1156; f) E. van Lenthe, E. J. Baerends, J. G. Snijders, *J. Chem. Phys.* **1994**, *101*, 9783–9792; g) E. van Lenthe, A. Ehlers, E. J. Baerends, *J. Chem. Phys.* **1999**, *110*, 8943–8953.
- [13] a) T. A. Albright, J. K. Burdett, M.-H. Whangbo, *Orbital Interactions in Chemistry*, John Wiley & Sons, Inc., **2013**; b) F. M. Bickelhaupt, E. J. Baerends, in *Reviews in Computational Chemistry*, Vol. 15 (Eds.: K. B. Lipkowitz, D. B. Boyd), Wiley-VCH, New York, **2000**, pp. 1–86; c) T. A. Hamlin, P. Vermeeren, C. Fonseca Guerra, F. M. Bickelhaupt, in *Complementary Bonding Analyses* (Ed.: S. Grabowski), De Gruyter, Berlin, **2021**, pp. 199–212; d) R. van Meer, O. V. Gritsenko, E. J. Baerends, *J. Chem. Theory Comput.* **2014**, *10*, 4432–4441.
- [14] a) C. Fonseca Guerra, J. W. Handgraaf, E. J. Baerends, F. M. Bickelhaupt, *J. Comput. Chem.* **2004**, *25*, 189–210; b) C. Nieuwland, P. Vermeeren, F. M. Bickelhaupt, C. Fonseca Guerra, *J. Comput. Chem.* **2023**, *44*, 2108–2119.
- [15] a) F. M. Bickelhaupt, K. N. Houk, *Angew. Chem. Int. Ed.* **2017**, *56*, 10070–10086; b) P. Vermeeren, T. A. Hamlin, F. M. Bickelhaupt, *Chem. Commun.* **2021**, *57*, 5880–5896; c) P. Vermeeren, S. C. C. van der Lubbe, C. Fonseca Guerra, F. M. Bickelhaupt, T. A. Hamlin, *Nature Protoc.* **2020**, *15*, 649–667.
- [16] C. Fonseca Guerra, Z. Szekeres, F. M. Bickelhaupt, *Chem. Eur. J.* **2011**, *17*, 8816–8818.

Manuscript received: November 11, 2023
Revised manuscript received: December 11, 2023
Accepted manuscript online: December 11, 2023
Version of record online: January 15, 2024